The Influence of the Skin Effect on the Amplitude of Single Pulse Gamma Detected NMR on Oriented Nuclei Signals

D. J. Isbister and D. H. Chaplin *

Department of Physics, University College, The University of New South Wales, Australian Defence Force Academy, Canberra, ACT, Australia

Z. Naturforsch. **45a**, 43–49 (1990); received July 7, 1989

The effects of skin depth on gamma detected single pulse Nuclear Magnetic Resonance on Oriented Nuclei (NMRON) signals are theoretically explored for narrow, intermediate and broad line metallic samples, using the density matrix approach describing a pure Zeeman system. It is shown that the skin effect distortion of the signal can dominate over intermediate to broadline distortions for that range of experimental conditions generally applicable to ferromagnetic hosts. In particular, the skin effect distortions of the first maximum, obtained when the excitation pulse width is lengthened, are significant and can determine the accuracy of calibration of the radiofrequency "(rf)" field amplitude at the resonating nuclei when assigning an average turn angle to this maximum.

Key words: NMRON, Zeeman interactions, Skin effect, Density matrix.

1. Introduction

The first applications of pulsed NMRON [1] using gamma detection were on ferromagnetic metal hosts, primarily because of the ease of cooling the metals and the large magnetic hyperfine fields available at most impurity sites. Single pulse and three pulse spin echo NMRON signals were generally investigated, the former serving as a precursor calibration experiment when the fractional change in gamma anisotropy was followed as a function of the pulse width [2]. The appearance of a weak first maximum in this response over a typical range of pulse widths from 0.1 to 1.5 μs was interpreted as an average turn angle of approximately 90°, a situation strictly true only in the limit of narrow line, zero skin effect samples. The distortion and displacement of this calibration maximum as a function of line broadening was thoroughly explored by Cooke et al. [3] using a classical ensemble rotation approach applicable for a Zeeman system.

It is the purpose of this paper to examine, firstly in isolation, the effects of skin depth on the single pulse gamma detected signals for narrow line samples, and, secondly, to combine the effects of skin depth and intermediate-to-broad line distributions in order to allow realistic comparisons with pulsed NMRON experiments on inhomogeneously broadened ferromagnetic hosts. The experimental motivation for these theoretical studies was, that with better (e.g. single crystal) samples and radiofrequency transmission, the single pulse signals as a function of pulse width failed to develop towards the swings in amplitude predicted from the calculations due to Cooke et al. [3], which totally ignored skin effects.

We have chosen to perform these skin effect calculations using the density matrix approach in preparation for the introduction of quadrupole effects at a later date [4], although we have utilized the classical results of Cooke et al. [3] as a check on the correctness of an essentially equivalent but far more powerful approach. The omission of electric quadrupole interactions (EQI's) is entirely appropriate for light to intermediate mass impurities ($A < 150$) in cubic ferromagnets wherein the range of measured EQI's is known to be typically less than 20 kHz whereas the rf Zeeman interaction during the application of the single pulse is typically 250 kHz [1]. We have been strongly influenced by the methods adopted by Mehring [5], who performed the skin effect calculation first for the case of conventional pulsed NMR on high temperature, narrow line, metallic systems. In those calculations it was appropriate to follow the first rank detection tensor, $I_{\pm}$, corresponding to the rotating transverse nuclear magnetization inducing an emf in the

Reprint requests to Prof. D. H. Chaplin, Department of Physics, University College, The University of New South Wales, Australian Defence Force Academy, Northcott Drive, Campbell ACT 2600, Australia.

0932-0784 / 90 / 0100-0043 $ 01.30/0. – Please order a reprint rather than making your own copy.

transverse pickup coil. In our calculations, however, we must assume nuclear orientation conditions prior to the pulse, a forward skin effect only, and a detection tensor appropriate to the parity conserving characteristics of the nuclear electromagnetic interaction providing the gamma ray detection medium.

Throughout this paper we will assume that the NMRON signals are obtained at nuclear orientation temperatures sufficiently high that only the second order orientation parameter B_2 is necessary to describe the populations during thermal equilibrium and resonant excitation. It should be recalled, however, that for high spin nuclei ($I > 3/2$), the fractional changes in B_4 can be significant, and that this additional complication should not always be neglected.

2. Theory

In this section the density matrix approach will be detailed for gamma detected NMRON measurements resulting from a single pulse of resonant rf field. The response of a doped radioactive NMRON sample is modelled by the calculated response of a set of uniformly distributed resonating nuclear spins to a depth d within the metallic host crystal, interacting with the skin effect attenuated rf field. This model is entirely appropriate to thin foils wherein the host plus radioactivity have been melted together and then rolled, or the radioactivity has been diffused for many hours into the thin foil. For simplicity, we will assume that the same approach is broadly applicable to the case of bulk metals, lightly diffused. That is to say, we will ignore exponential and irregular diffusion profiles, interpreting d as the mean diffusion depth for such samples.

Mehring [5] has shown that this skin effect contribution to the conventional NMR high temperature signal significantly perturbs the traditional sinusoidal response both in magnitude and phase.

For γ-detected NMRON the gamma detector is placed along the z axis defined by the principal quantization axis of orientation.

In terms of the density matrix $\varrho(t)$ and the γ-anisotropy detection tensor $(I_z^2 - \mathbf{I}^2/3)$, the time dependent signal from the system is

$$S(t) \propto \mathrm{Tr}\,[\varrho(t)(I_z^2 - \mathbf{I}^2/3)]\,. \tag{1}$$

Equation (1) can be generalized to include contributions due to the interactions of spins located at a depth r relative to the surface of the metallic model: $S(t, r)$ is then the contribution to the total signal $S(t)$ from spins located at that distance r from the surface, and $\varrho(t, r)$ is the corresponding density matrix. The summation of these contributions $S(t, r)$ over the uniform distribution of nuclear spins is then $S(t)$, given now as the normalized integral

$$S(t) = \frac{\int_0^d \mathrm{d}r\, S(t, r)}{\int_0^d \mathrm{d}r\, S(t=0, r)}\,, \tag{2}$$

and

$$\varrho(t, r) = \exp\left\{-i \int_0^t \mathrm{d}t'\, \mathscr{H}(t')/\hbar\right\} \varrho(0, r) \exp\left\{i \int_0^t \mathrm{d}t'\, \mathscr{H}(t')/\hbar\right\}.$$

The significant part of the Hamiltonian, $\mathscr{H}$, which is responsible for the dynamics of an individual spin packet in the above model, can be written in the laboratory frame as

$$\mathscr{H} = \begin{cases} -\gamma\hbar(H_0 I_z + \boldsymbol{H}_1 \cdot \mathbf{I}) & \text{if} \quad 0 < t < t_\mathrm{p} \\ -\gamma\hbar H_0 I_z & \text{otherwise} \end{cases}. \tag{3}$$

$\boldsymbol{H}_1$ and H_0 are respectively the transverse rf field (pulsing) and longitudinal magnetic field (static orienting field) of the total Zeeman field $\boldsymbol{H} = (H_{1x}, H_{1y}, H_0)$; t_p is the duration of the pulse and $\mathbf{I}$ is the quantum nuclear spin operator.

The inhomogeneous broadening of internal magnetic fields in ferromagnets is described by a normalised distribution function $p(\omega_0 - \omega)$, where $\omega_0 = \gamma H_0$ and ω is the angular frequency associated with the transformation to the rotating frame. In the rotating frame the Hamiltonian of (3) becomes

$$\mathscr{H}' = \begin{cases} -\gamma\hbar\boldsymbol{H}_\mathrm{eff} \cdot \mathbf{I} & \text{if} \quad 0 < t < t_\mathrm{p} \\ -\gamma\hbar(H_0 - \omega/\gamma) I_z & \text{otherwise} \end{cases}, \tag{4}$$

with the effective magetic field $\boldsymbol{H}_\mathrm{eff}$ defined at the surface ($r = 0$), as

$$\boldsymbol{H}_\mathrm{eff} = H_1 \hat{\boldsymbol{y}} + (H_0 - \omega/\gamma)\, \hat{\boldsymbol{z}}\,, \tag{5}$$

and

$$\varrho'(t, r) = \exp(-i\mathscr{H}' t/\hbar)\, \varrho(0, r) \exp(i\mathscr{H}' t/\hbar). \tag{6}$$

Henceforth in this paper we shall omit the prime character in ϱ'. The rf field H_1 penetrates the surface to interact with those spins located at a depth r below the surface. Here the rf field can be written as the two

component vector

$$\boldsymbol{H}_1(r) = H_1(r=0)\, e^{-r/\delta}\, \hat{\boldsymbol{n}}_1(r), \tag{7}$$

where the changing direction of the rf field is defined by the unit vector $\hat{\boldsymbol{n}}_1(r)$

$$\hat{\boldsymbol{n}}_1(r) = (\sin(r/\delta), \cos(r/\delta), 0) \tag{8}$$

with δ being the skin depth asociated with the metallic model.

The Zeeman form of the propagators in (3) leads for all spins to the pure rotations $\mathrm{Rot}(\beta(r), \xi(r))$ through various angles $\beta(r)$ about various axes $\xi(r)$. For the surface resonant rf field, assumed in (7) to be directed along the y' axis of the rotating frame at $r=0$, the $\xi(r)$ rotational axis reduces simply to the y' direction of the rf field, and the associated rotation becames $\mathrm{Rot}(\beta(r), \xi(r)) = \mathrm{Rot}(\beta_0, y')$ with $\beta_0 = \gamma H_1(r=0)\, t_p$ being the traditionally defined rotational angles of the surface ($r=0$) spins. Straightforward evaluation of the propagator using (4)–(8) is unwieldy, and the incorporation of the changes due to the skin effect on spins beneath the surface is accomplished for the resonance case ($H_0 - \omega/\gamma = 0$) through the identity $\mathrm{Rot}(\beta(r), \xi(r)) = \mathrm{Rot}(\beta(r), \hat{n}_1(r))$ and

$$\mathrm{Rot}(\beta(r), \xi(r)) = \exp(-i\phi I_{z'}) \exp(i\beta(r) I_{y'}) \exp(i\phi I_{z'}), \tag{9}$$

where

$$\phi = r/\delta,$$
$$\beta(r) = \gamma H_1(r=0)\, t_p\, e^{-r/\delta} = \beta_0\, e^{-r/\delta}.$$

For notational convenience we shall henceforth write the operator Rot as R [6].

2.1. *On-Resonance Case* ($(H_0 - \omega/\gamma) = 0$) *for the Single Spin Packet*

The precessional motion of the off-resonance spins about the effective field in the rotating frame of reference complicates the evaluation of the signal in (2) using (4)–(8), and the derivation of $S(t)$ for the simpler on-resonance ($H_0 - \omega/\gamma = 0$) case will be detailed first in this section.

The contributions to the expectation value of $(I_z^2 - \mathbf{I}^2/3)$ at time $t = t_p$ from spins distant r from the surface is

$$\langle I_z^2 - \mathbf{I}^2/3 \rangle_r = \mathrm{Tr}[\varrho(t_p, r)(I_z^2 - \mathbf{I}^2/3)], \tag{10}$$

where substitution of the Zeeman propagators and $R(\beta(r), \hat{n}_1(r))$ in the density matrix evaluated at $t = t_p$ gives

$$\begin{aligned}\varrho(t_p, r) &= R(\beta(r), \hat{n}_1(r))\, \varrho(0, r)\, R(\beta(r), \hat{n}_1(r))^{-1} \\ &= e^{-i\phi I_{z'}}\, e^{i\beta(r) I_{y'}}\, e^{i\phi I_{z'}}\, \varrho(0, r)\, e^{-i\phi I_{z'}} \\ &\quad e^{-i\beta(r) I_{y'}}\, e^{i\phi I_{z'}}.\end{aligned} \tag{11}$$

The notation $\langle I_z^2 - \mathbf{I}^2/3 \rangle_r$ is introduced to denote a contribution to an average $(I_z^2 - \mathbf{I}^2/3)$ from spins at a distance r within the sample. Direct evaluation of (10) gives

$$\begin{aligned}\langle I_z^2 - \mathbf{I}^2/3 \rangle_r = \sum_{m=-I}^{I} &(m^2 - I(I+1)/3) \\ &\langle m | e^{i\beta(r) I_{y'}}\, e^{i\phi I_{z'}}\, \varrho(0, r)\, e^{-i\phi I_{z'}}\, e^{-i\beta(r) I_{y'}} | m \rangle,\end{aligned} \tag{12}$$

which can be further simplified by the closure identity $\mathbf{1} = \sum_{m=-I}^{I} |m\rangle\langle m|$ being used to evaluate the effect of the operators on each side of $\varrho(0, r)$ in the right hand side of (12). Then the contribution to the average anisotropy tensor from nuclear spins found at a distance r from the surface of the model metal is

$$\begin{aligned}\langle I_z^2 - \mathbf{I}^2/3 \rangle_r = \sum_m \sum_{m_1} \sum_{m_2} &(m^2 - I(I+1)/3)\, d^i_{m m_1}(\beta(r)) \\ &d^i_{m m_2}(\beta(r))\, \langle m_1 | \varrho(0, r) | m_2 \rangle\, e^{i(m_1 - m_2)\phi},\end{aligned} \tag{13}$$

where $d^i_{mn}(\beta) = \langle m | e^{-i\beta I_{y'}} | n \rangle$ has been substituted. The initial conditions for the density matrix are now assumed to be proportional to I_z^2, with the resulting replacement of the elements $\langle m_1 | \varrho(0, r) | m_2 \rangle$ by $m_1^2\, \delta_{m_1 m_2}$ on the right hand side of (13) leading to

$$\begin{aligned}\langle I_z^2 - \mathbf{I}^2/3 \rangle_r = \sum_m \sum_{m_1} &(m^2 - I(I+1)/3)\, m_1^2 \\ &d^i_{m m_1}(\beta(r))\, d^i_{m m_1}(\beta(r)).\end{aligned} \tag{14}$$

When the factors m^2 and m_1^2 are replaced by their equivalent 3-j symbols $\begin{pmatrix} i & i & 2 \\ m_1 & -m_1 & 0 \end{pmatrix}$, (14) can be shown in the limiting case of $\delta \to \infty$ to be equivalent to the classical ensemble results of Cooke et al. [3] for their infinitely hard pulse S_2 signal.

In contrast to Kotzur's et al. analysis [5], there is no phase factor of $e^{i\phi}$ present on the right hand side of (14) due to the axial nature of the detector tensor. Also, further attenuation of $\langle I_z^2 - \frac{1}{3}\mathbf{I}^2 \rangle_r$ by a backward skin effect is not required in the experimental detection of γ anisotropy NMRON signals because of the decoupling between the gamma photons and the rf excitation. For the on-resonance condition being considered here, the final signal of (2) can be written

$$S(t_p) = N^{-1} \sum_{m, m_1} (m^2 - I(I+1)/3)\, m_1^2 \int_0^d \mathrm{d}r\, (d^i_{m m_1}(\beta(r)))^2, \tag{15}$$

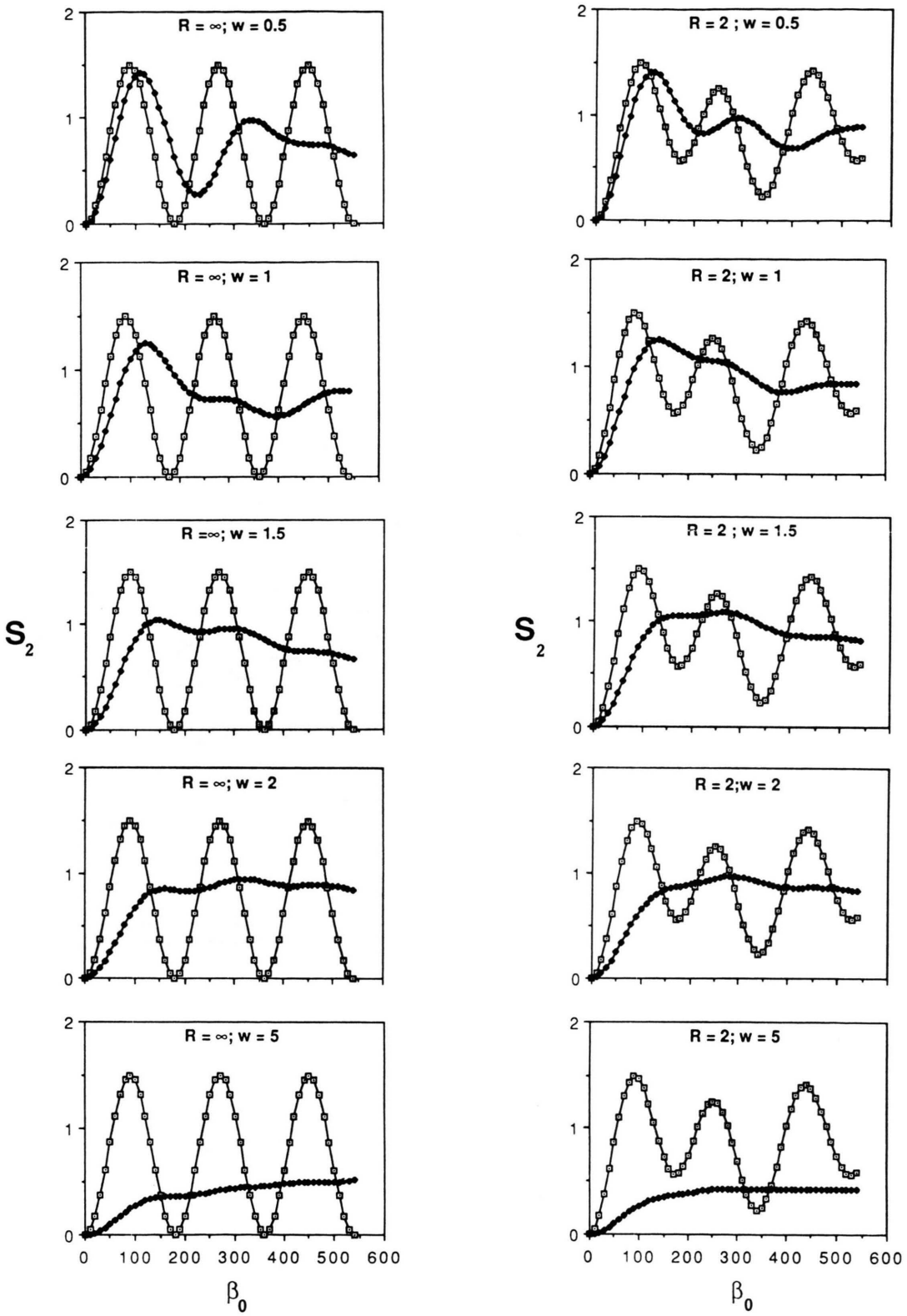

Fig. 1. Calculated single pulse NMRON signals versus surface turn angle β_0 for narrow line ($R=\infty$) and intermediate ($R=2.0$) resonances and various $w=d/\delta$. The curves marked by the open squares represent the $w=0$ results (equivalent to Cooke et al. [3]) while those marked by the black diamonds represent the skin effect results.

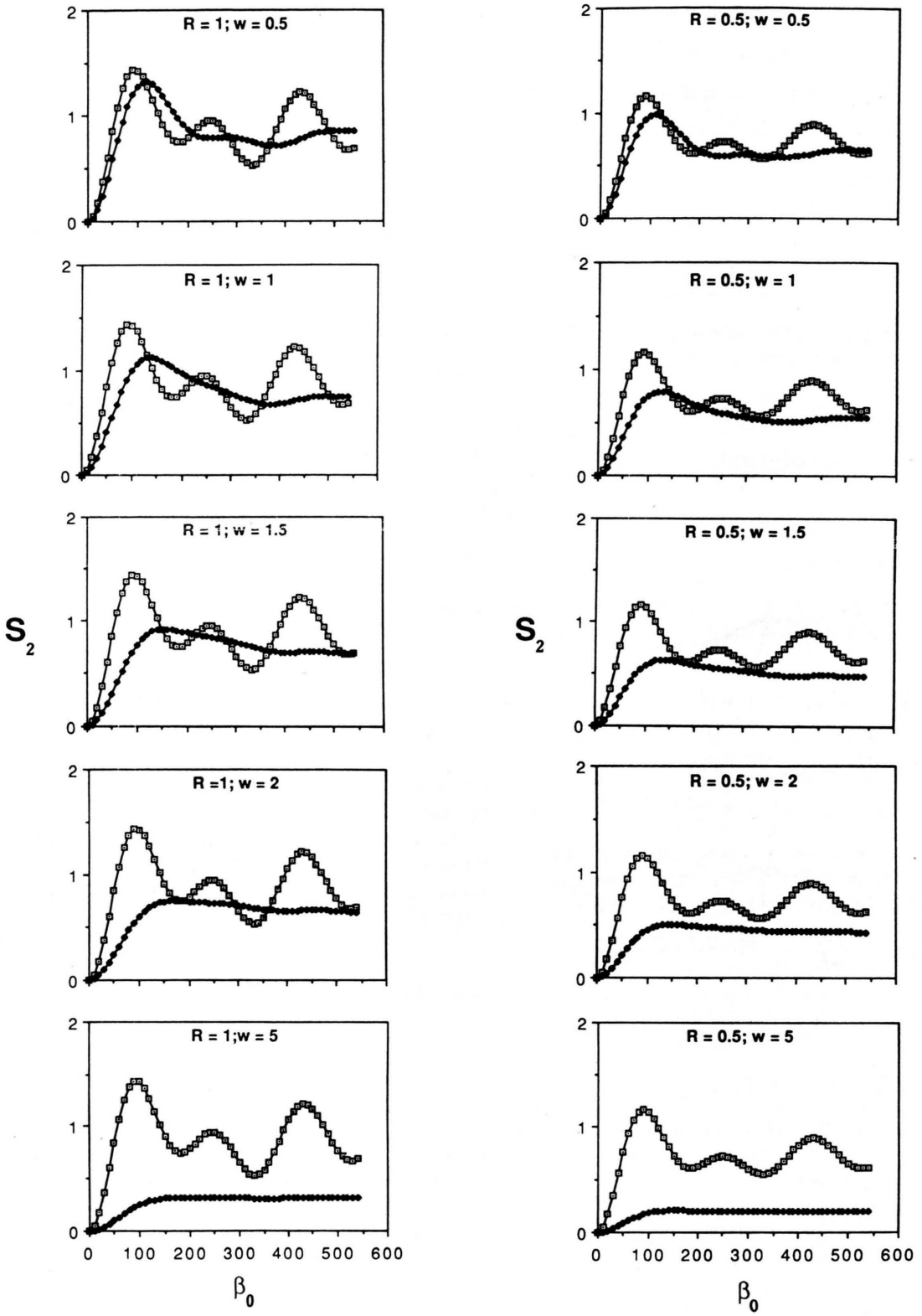

Fig. 2. Calculated single pulse NMRON signals versus surface turn angle β_0 for intermediate to broadline ($R=1.0$, 0.5) resonances and various $w=d/\delta$. The curves marked by the open squares represent the $w=0$ results (equivalent to Cooke et al. [3]) while those marked by the black diamonds represent the skin effect results.

where the normalization factor is

$$N=(2I-1)(2I)(2I+1)(2I+2)(2I+3)\,d/180\,. \quad (16)$$

For arbitrary I, the right hand side of (15) may be evaluated as

$$S(t_p)=\frac{1}{d}\int_0^d dr(\cos^2\beta(r)-1/3)\,. \quad (17)$$

2.2. *Off Resonance Case* ($(H_0-\omega/\gamma)\neq 0$)

For $(H_0-\omega/\gamma)\neq 0$, the nuclear spins precess about the effective magnetic field H_{eff} in time t by the angle $\omega_{\text{eff}}\,t$, where

$$\omega_{\text{eff}}=\sqrt{(\gamma H_1(r))^2+(\gamma H_0-\omega)^2}\,. \quad (18)$$

The rotation associated with such precessional motion is given by

$$R(\omega_{\text{eff}}\,t, H_{\text{eff}})=R(-\phi+\pi/2, z')^{-1}\,R(\theta_{\text{eff}}\,y')^{-1}\,R(\omega_{\text{eff}}\,t, z')\,R(\theta_{\text{eff}}, y')\,R(-\phi+\pi/2, z'), \quad (19)$$

where $\tan\theta_{\text{eff}}=\gamma H_1(r)/(\gamma H_0-\omega)$. The density matrix for the off-resonance case can be written in terms of $R(\omega_{\text{eff}}\,t_p, H_{\text{eff}})$ and $\phi_{\text{eff}}=\omega_{\text{eff}}\,t_p$ as

$$\varrho(t_p, r)=R(\phi_{\text{eff}}, H_{\text{eff}})\,\varrho(0, r)\,R(\phi_{\text{eff}}, H_{\text{eff}})^{-1} \quad (20)$$

$$=e^{-i(\phi-\pi/2)I_{z'}}\,e^{-i\theta_{\text{eff}}I_{y'}}\,e^{i\phi_{\text{eff}}I_{z'}}\,e^{i\theta_{\text{eff}}I_{y'}}\,e^{i(\phi-\pi/2)I_{z'}}\,\varrho(0, r)\,e^{-i(\phi-\pi/2)I_{z'}}\,e^{-i\theta_{\text{eff}}I_{y'}}\,e^{-i\phi_{\text{eff}}I_{z'}}\,e^{i\theta_{\text{eff}}I_{y'}}\,e^{i(\phi-\pi/2)I_{z'}}\,. \quad (21)$$

The extension of the previous analysis to off-resonance conditions and a "softer" pulse is straightforward, and the analysis leading to (14) becomes

$$\langle I_z^2-\mathbf{I}^2/3\rangle_r=\sum_{m_1,m_2,m_3,m_4}(m_1^2-I(I+1)/3)\,m_3^2\;e^{i\omega_{\text{eff}}t_p(m_2-m_4)}\,d_{m_1m_2}^{i}(\theta_{\text{eff}})\,d_{m_3m_2}^{i}(\theta_{\text{eff}})\,d_{m_3m_4}^{i}(\theta_{\text{eff}})\,d_{m_1m_4}^{i}(\theta_{\text{eff}})$$

$$=(2l+1)^{-1}\,D_{00}^{2*}(\omega_{\text{eff}}\,t_p, \theta_{\text{eff}}, 0). \quad (22)$$

In this equation the representation of the rotation group $D_{mn}^{l}(\alpha, \beta, \gamma)$, has been introduced and is defined as

$$D_{mn}^{l}(\alpha, \beta, \gamma)=\langle m|\exp(-i\alpha I_{z'})\exp(-i\beta I_{y'})\exp(-i\gamma I_{z'})|n\rangle \quad (23)$$

The result of (22) is linearly related to the classical ensemble results of Cooke et al. [3] for S_2 when the factors corresponding to the skin effect are set equal to zero (i.e. $\delta\to\infty$): $S_2=1-\frac{3}{2}\langle I_z^2-\mathbf{I}^2/3\rangle_r$. It can also be shown that

$$\langle 0|R_{\text{eff}}(\omega_{\text{eff}}\,t_p)|0\rangle=P_l(\cos^2\theta_{\text{eff}}+\sin^2\theta_{\text{eff}}\cos\omega_{\text{eff}}\,t_p). \quad (24)$$

The signal associated with the calculation for the off-resonance condition can be finally expressed in the format of (17) as

$$S(t_p, \Omega)=\frac{1}{d}\int_0^d dr(\cos^2(\beta(r, \Omega))-1/3), \quad (25)$$

where

$$\beta(r, \Omega)=t_p\sqrt{(\gamma H_1(r=0)\,e^{-r/\delta})^2+(\gamma H_0-\omega)^2} \quad (26)$$

$$=\beta_0\sqrt{e^{-2r/\delta}+((\omega_0-\omega)/\omega_1)^2}\,, \quad (27)$$

and β_0 is the previously defined "turn angle" associated with spins at the surface, $\omega_1=\gamma H_1(r=0)$, and $\omega_0=\gamma H_0$. Due to the inhomogeneous broadening intrinsic to the metal, this signal must be averaged over the corresponding frequency distribution $p(\Omega)=p(\omega_0-\omega)$ about a central resonant frequency of the whole lineshape. If this is done, then the final signal is

$$S(t_p)=\int_{-\infty}^{\infty}d\Omega\,p(\Omega)\,S(t_p, \Omega) \quad (28)$$

$$=\frac{1}{d}\int_{-\infty}^{\infty}d\Omega\,p(\Omega)\int_0^d dr(\cos^2\beta(r, \Omega)-1/3), \quad (29)$$

and $p(\Omega)=(\ln 2/\pi\Delta^2)^{1/2}\exp(-\ln 2\,\Omega^2/\Delta^2)$ characterises the spread of the frequency distribution, where Δ is the halfwidth of the distribution measured at half maximum of the assumed Gaussian distribution. Equation (29) can be evaluated numerically using trapezoidal rules for the r and Ω integrations.

3. Results and Discussion

Figure 1 includes the single pulse gamma NMRON signals for narrow line ($R=\infty$) resonances as a function of the dimensionless parameter $w=d/\delta$. Significant features are

1. the loss of large oscillatory swings in the time evolution of the signal as a function of turn angle (experimentally, the pulse width) for $w\geqq 0.5$.
2. the lateral displacement of the first maximum to larger turn angles by as much as a factor of two, for $w\geqq 0.5$. It is this feature that is most relevant for sensible calibration of the internally enhanced rf field.

Figures 1 and 2 show the single pulse gamma NMRON signals for intermediate-to-broad line resonances as described by the dimensionless ratio $R=\omega_1/\Delta$. The combined effects in Fig. 2 serve not only to attenuate the oscillations more severely but produce significantly diminished limiting signals at high turn angles which should prove useful for comparison with experiment provided non-resonant heating effects are negligible at the larger turn angles.

In an effort to understand the severity of the skin effect in damping out the oscillation, a detailed examination of the integrand of $S_2=1-\frac{3}{2}S(t_p)$ as a function of r was undertaken. It was found that the integrand provided two broad classes of response with respect to β_0 angles below and above about $\beta_0 \sim 120°$ (20). For the small β_0 region the integrand of S_2 is given by an exponentially decreasing function of r across all diffusion zones (defined in terms of units of δ from the surface). For β_0's above 120° the integrand achieves a maximum within the first diffusion zone ($r \leqq \delta$) before monotonically decreasing at a significantly slower rate beyond $r=\delta$. The combination leads to the featureless and slower rise to a weaker first maximum for $w \geqq 1$, and for intermediate to broad line resonances the almost complete loss of the first maximum. For larger β_0's (above 300°) cancellations occur between contributions from rapidly oscillating integrands within the first zone, which leads to the featureless high turn angles limiting signals of Figs. 1 and 2 for $w > 1$. The amplitudes of the rapidly oscillating larger β_0 integrands are successively diminished for decreasing R values whereas the exponential decay of the small β_0 response is not nearly so sensitive to the effect of decreasing R. These contributions to the integrand for different β_0 values can also be used to detail the w dependence of the signal (from a consideration of a single plot of the integrand for various values of the β_0's over the maximum range for $r=5\delta$) provided the contributions from each individual zone are correctly weighted by the number fraction of spins located within each zone. For the uniform distribution of spins considered in this model this is simply proportional to the inverse of the number of zones appropriate to the value of w.

4. Conclusions

It has been shown that for pulsed NMRON signals from metallic ferromagnets the inclusion of skin effect distortions is necessary to enable the correct assignment of the average turn angle for a given pulse width – and hence the sensible calibration of the internally enhanced radiofrequency field. Detailed comparisons with experimental results will be published elsewhere, as well as further theoretical calculations for the triple pulse spin echo NMRON signal with skin depth effects included.

Acknowledgements

The authors wish to thank Dr. W. D. Hutchison for a critical reading of the manuscript. One of us (D. H. Chaplin) acknowledges the support of the Australian Research Council.

[1] D. H. Chaplin and G. V. H. Wilson, in: Low Temperature Nuclear Orientations (N. J. Stone and H. Postma, eds.), Chapt. 14, Elsevier Science Publishers 1986.
[2] See for example: P. J. Back, D. H. Chaplin, H. R. Foster, G. A. Stewart, and G. V. H. Wilson, Hyp. Int. **22,** 193 (1985).
[3] P. Cooke, D. H. Chaplin, and G. V. H. Wilson, J. Phys. **C 12,** 595 (1979).
[4] P. T. Callaghan, P. J. Back and D. H. Chaplin, Quadrupole Modulation of Spin Echoes in Nuclear Magnetic Resonance of Oriented Nuclei, in preparation.
[5] D. Kotzur, M. Mehring, and O. Kanert, Z. Naturforsch. **28 a,** 1607 (1973), and references therein.
[6] V. Heine, Group Theory in Quantum Mechanics, Pergamon Press, Oxford 1964.